

Alma Mater Studiorum Università di Bologna
Archivio istituzionale della ricerca

Electrical Stimulation by an Organic Transistor Architecture Induces Calcium Signaling in Nonexcitable Brain Cells

This is the final peer-reviewed author's accepted manuscript (postprint) of the following publication:

Published Version:

Borrachero-Conejo, A.I., Saracino, E., Natali, M., Prescimone, F., Karges, S., Bonetti, S., et al. (2019). Electrical Stimulation by an Organic Transistor Architecture Induces Calcium Signaling in Nonexcitable Brain Cells. *ADVANCED HEALTHCARE MATERIALS*, 8(3), 1-12 [10.1002/adhm.201801139].

Availability:

This version is available at: <https://hdl.handle.net/11585/661604> since: 2019-02-07

Published:

DOI: <http://doi.org/10.1002/adhm.201801139>

Terms of use:

Some rights reserved. The terms and conditions for the reuse of this version of the manuscript are specified in the publishing policy. For all terms of use and more information see the publisher's website.

This item was downloaded from IRIS Università di Bologna (<https://cris.unibo.it/>).
When citing, please refer to the published version.

(Article begins on next page)

This is the final peer-reviewed accepted manuscript of:

Borrachero-Conejo AI, Saracino E, Natali M, Prescimone F, Karges S, Bonetti S, Nicchia GP, Formaggio F, Caprini M, Zamboni R, Mercuri F, Toffanin S, Muccini M, Benfenati V. Electrical Stimulation by an Organic Transistor Architecture Induces Calcium Signaling in Nonexcitable Brain Cells. *Adv Healthc Mater.* 2019 Feb;8(3):e1801139. doi: 10.1002/adhm.201801139. Epub 2018 Dec 19. PMID: 30565894.

The final published version is available online at:
<https://onlinelibrary.wiley.com/doi/full/10.1002/adhm.201801139>

Rights / License:

The terms and conditions for the reuse of this version of the manuscript are specified in the publishing policy. For all terms of use and more information see the publisher's website.

This item was downloaded from IRIS Università di Bologna (<https://cris.unibo.it/>)

When citing, please refer to the published version.

DOI: 10.1002/ (please add manuscript number)

Article type: Full Paper

Electrical stimulation by an organic transistor architecture induces calcium signalling in non-excitable brain cells

A.I. Borrachero-Conejo, E. Saracino, M. Natali, F. Prescimone, S. Karges, S. Bonetti^{o1}, G. P. Nicchia, F. Formaggio, M. Caprini, R. Zamboni, F. Mercuri, S. Toffanin*, M. Muccini*, and V. Benfenati*

A. I. Borrachero-Conejo, M. Natali, F. Prescimone, Dr. S. Karges, S. Bonetti

F. Mercuri, Dr. S. Toffanin, and M. Muccini

Consiglio Nazionale delle Ricerche (CNR) Istituto per lo Studio dei Materiali Nanostrutturati (ISMN) via Gobetti, 101, 40129, Bologna, Italy.

E. Saracino, R. Zamboni and V. Benfenati

Consiglio Nazionale delle Ricerche (CNR) Istituto per la Sintesi Organica e la Fotoreattività (ISOF) via Gobetti, 101, 40129, Bologna, Italy

G. P. Nicchia.

University of Bari Aldo Moro, Dipartimento di Bioscienze, Biotecnologie e Biofarmaceutica, Via Edoardo Orsini, 70125 Bari, Italy

M. Caprini and F. Formaggio

* Present address: Cell dynamics s.r.l. via Gobetti, 101, 40129, Bologna, Italy

This is the author manuscript accepted for publication and has undergone full peer review but has not been through the copyediting, typesetting, pagination and proofreading process, which may lead to differences between this version and the [Version of Record](#). Please cite this article as [doi: 10.1002/adhm.01801139](#).

This article is protected by copyright. All rights reserved.

University of Bologna, Dipartimento di Farmacia e Biotecnologie (FaBit), via San Donato 15, Bologna, Italy

e-mail: valentina.benfenati@isof.cnr.it; m.muccini@bo.ismn.cnr.it; s.toffanin@bo.ismn.cnr.it

Keywords: (astrocytes, organic devices, bioelectronics, ion channels, calcium signaling)

Abstract

Organic bioelectronics has a huge potential to generate interfaces and devices for the study of brain functions and for the therapy of brain pathologies. In this context, increasing efforts are needed to develop technologies for monitoring and stimulation of non-excitabile brain cells, called astrocytes. Astroglial calcium signalling play, indeed, a pivotal role in the physiology and pathophysiology of the brain. In this work, we demonstrate the use of transparent Organic Cell Stimulating and Sensing Transistor (O-CST) architecture, fabricated with N, N'-ditridecylperylene-3,4,9,10-tetracarboxylic diimide (P13), to elicit and monitor intracellular calcium concentration ($[Ca^{2+}]_i$) in primary rat neocortical astrocytes. The transparency of O-CST allowed performing calcium imaging experiments showing that extracellular electrical stimulation of astrocytes induces a drastic increase in $[Ca^{2+}]_i$. Pharmacological studies indicate that Transient Receptor Potential (TRP) superfamily, are critical mediators of the $[Ca^{2+}]_i$ increase. Experimental and computational analyses shows that $[Ca^{2+}]_i$ response is enabled by the O-CST device architecture. Noteworthy, the extracellular field application induces a slight but significant increase in the cell volume. Collectively, we show that the O-CST is capable to selectively evoke astrocytes $[Ca^{2+}]_i$, paving the way to the

development of organic bioelectronic devices as glial interfaces to excite and control physiology of non-neuronal brain cells.

1. Introduction

The unravelled issues related to mechanisms underpinning brain function have tremendously increased the demand of bioelectronic devices enabling the monitoring and dialogue with brain cells to modulate their physiology. Organic semiconducting materials display intrinsic multifunctionality, combining iono-electronic transport properties, photonic properties and optical transparency within the visible range with improved biocompatibility with neural cells compared to inorganic substrates.^[1-4] Notably, the survival of primary neuronal cells on organic bioelectronic polymers^[1,3,4] and small molecules^[5,6] is higher when compared to silicon/glass substrates, while the functionality of brain cells is preserved on organic biofunctional interfaces.^[1,5] Importantly, organic bioelectronic^[3,7] and bio-optoelectronic^[8,9] devices capable to record, stimulate and modulate functionality of neuronal cells *in vitro*^[7] and *in vivo*^[3] have been reported, showing the potential and the relevance for clinical neurology as well as for neuroscience fundamental studies.

Recently, the role of glial cells, called astrocytes, is emerging among the challenges and targets that need to be considered for the development of devices devoted to neuroscience investigations and applications. Astrocytes are, indeed, the cells that are majorly involved in the regulation of the concentration of ions and neurotransmitters in the synaptic cleft, participating to communication signals between neurons and playing a pivotal role in the

brain physiology.^[10,11] The function of astrocytes mainly depends on the activity of transmembrane proteins forming transporters, ion channels and aquaporins.^[12] Moreover, astrocytes are capable to respond to different extracellular chemophysical stimuli (such as neurotransmitters, temperature, osmotic gradient, mechanical stimulus) by variation in their cytosolic Ca^{2+} concentrations ($[\text{Ca}^{2+}]_i$).^[13,14] Interestingly, *in vivo* studies indicated that $[\text{Ca}^{2+}]_i$ oscillations and dynamics can occur in a selective district (microdomain) or spread between astroglial cells through gap junctions (Ca^{2+} waves).^[15,16] The increase in $[\text{Ca}^{2+}]_i$ can be caused by the entry of extracellular Ca^{2+} or by the mobilization of the Ca^{2+} stored in the endoplasmic reticulum.^[14] Extracellular Ca^{2+} can mainly enter into the cell via ionotropic channels, such as the purinergic receptor P2X_7 ^[17], and through members of the Transient Receptor Potential (TRP) family, that includes Transient Receptor Potential Vanilloid 4 (TRPV4) and TRPA1.^[18,19] On the other hand, the release of Ca^{2+} from the intracellular stores is mediated by inositol 1,4,5- trisphosphate (IP_3), after activation of metabotropic receptors expressed on astrocytes membrane.^[14,20] Astroglial $[\text{Ca}^{2+}]_i$ signalling occurs at synaptic level in the cortex, where astrocytes enwrap almost 90% of pre- and post-synaptic neurons, in the so-called tripartite synapse.^[21] These findings led to the intriguing hypothesis of their involvement in cognitive functions.^[22] The pathophysiological implications of alteration in astroglial $[\text{Ca}^{2+}]_i$ oscillations are even more relevant. Indeed, aberrant Ca^{2+} signalling has been shown to be implicated in many pathological conditions such as Alzheimer's disease^[23], Down syndrome^[24], epilepsy^[25], brain tumours^[26] and ischemia.^[27] Notably, recent *in vivo* evidence reported that transcranial Direct Current Stimulation (tDCS) induces large-amplitude astroglial Ca^{2+} increase across the cortex, in mouse brain.^[28] In this view, even

though they are non-excitabile, i.e. not capable to generate action potentials, astroglial bioelectrical/biochemical signals are emerging as brand new target for the development of bioelectronic devices aiming at understanding/modulating brain functionality and dysfunction.^[29–32] However, despite the potential of organic electronics for neuroscience and the importance of astrocytes for brain physiology and pathology there is a lack of evidence that organic bioelectronic devices are capable to alter $[Ca^{2+}]_i$ signals in astrocytes by application of an electric field.

In our previous work, we have demonstrated that a bottom gate top contact organic cell stimulating and sensing transistor (O-CST) architecture fabricated with N, N'-ditridecylperylene-3,4,9,10-tetracarboxylic diimide (P13) has the ability to stimulate and record primary neurons from dorsal root ganglion (DRG) cell culture.^[7] Here we sought to verify the effect of extracellular stimulation, obtained by subthreshold operation of O-CST, on $[Ca^{2+}]_i$ signals in primary rat neocortical astrocytes.

We found that primary astroglial cells can adhere and grow over long term on thin films of P13, the capping layer of the O-CST. Taking advantage of the optical transparency of the O-CST, we established by Fluo-4 calcium imaging, that the extracellular electrical stimulation delivered by O-CST evokes intracellular calcium response in astrocytes. The pharmacological profile of the observed signal indicated that TRP channels are involved in the effect. By means of modelling and experimental data we also clarified the mechanism underpinning O-CST stimulation, revealing that the device architecture, structure and functionality are essential to achieve the observed activation in stimulated astrocytes.

Our study is the first demonstration of an organic device capable to evoke by electrical field calcium signalling in non-excitabile brain cells. Considering the growing importance of astrocytes in human physiology and pathology, our work sets the scene for the development of future glial interfaces.

2. Experimental Session

2.1 Cell culture preparations. All animal experiments were authorized by a local bioethical committee (Protocol n° 715/2016) and performed according to the Italian and European Council laws on animal use for experimental purposes. Experiments carried out with animals were performed in concordance to the European Council Law for the protection of laboratory animals, with the approval of the bioethical committee of the University of Bologna.

Primary cultures of pure cortical rat astrocytes were prepared as previously described.^[33] Briefly, after removing the meninges, the cerebral cortices of one to two-days-old Sprague-Dawley pups (P0-P2) were mechanically dissociated and placed in cell culture flasks containing DMEM-Glutamax medium supplemented with 15% fetal bovine serum (FBS), 100 U/ml penicillin and (100 mg/ml) streptomycin (all products were purchased from Gibco-Invitrogen, Milan, Italy). Culture flasks were maintained in a humidified atmosphere incubator at 37°C and 5% CO₂ for three to five weeks. The culture medium was replaced

every three days. Before medium change, flasks were gently shaken in order to detach microglial cells seeded on top of the astrocytic monolayer.^[34] At confluence, astroglial cells were enzymatically dispersed using trypsin–EDTA. Glass coverslips, P13 coated coverslips and OCST substrates were treated for 20 min with poly-D-lysine (PDL, 0.1 mg/ml in PBS). Cells were then seeded at the concentration of 80×10^4 cells per substrate and maintained in culture medium containing 10% FBS.

2.2 Cell viability assays. Cell viability was investigated by fluorescein diacetate (FDA) assay. The FDA (Sigma, Milan, Italy) stock solution (5 mg/ml) was prepared in acetone and 3.3 μ L of the stock solution was mixed with 1 mL of phosphate buffered saline (PBS). Astrocytes plated on PDL coated glass, P13 films coated with PDL and O-CST devices were incubated for 5 min at room temperature (22–24°C), washed with PBS and characterized by Nikon eclipse 80i fluorescent inverted microscope, equipped with a 20X objective. At least 10 image per sample were collected with a field of view of 900 μm^2 . Living cells were counted and the number of cells/area was calculated and compared at each considered time point.

2.3 O-CST fabrication. O-CST devices were fabricated in top-contact and bottom-gate configuration with an additional layer of organic semiconducting material on top of the contacts. The substrates consisted of glass coated with a 150 nm thick layer of sputtered Indium Tin Oxide (ITO). Before deposition the substrates were cleaned by multiple sonications in acetone 99.5% (Scharlau, Milan, Italy) and 2-propanol 99.5% (Sigma, Milan, Italy). 420 nm of PMMA (ALLRESIST GmbH, Strausberg, Germany) were deposited on top of the ITO layer by spin-coating in air and annealed for 12 h at 120 °C in vacuum. The 15 nm

thick P13 thin film was grown by sublimation under high vacuum at a base pressure of 10^{-6} mbar in an Edwards 306 sublimation chamber at a rate of 0.1 \AA s^{-1} . 30 nm thick gold electrodes were deposited in high vacuum at a pressure of $3\text{--}4 \times 10^{-6}$ mbar at a growth rate of 0.1 nm s^{-1} . The channel length between two gold electrodes was set to $70 \text{ }\mu\text{m}$. A 50 nm thick P13 capping layer was vacuum sublimed on top of the gold electrodes under the same conditions as described before.

2.4 Diode fabrication. Diodes were fabricated on the same cleaned glass substrates used for the O-CST devices, where no ITO was deposited. 420 nm of PMMA were deposited on top of the glass through spin-coating in air and annealed for 12h at 120°C in vacuum. The 15 nm thick P13 thin film was grown by sublimation under high vacuum at a base pressure of 10^{-6} mbar in an Edwards 306 sublimation chamber at a rate of 0.1 \AA s^{-1} . 20 nm thick gold electrode was deposited in high vacuum at a pressure of $3\text{--}4 \times 10^{-6}$ mbar at a growth rate of 0.1 nm s^{-1} . A 50 nm thick P13 capping layer was vacuum sublimed on top of the gold electrode under the same conditions as described before.

2.5 Calcium microfluorometry. Variations in the intracellular free Ca^{2+} concentration ($[\text{Ca}^{2+}]_i$) were monitored by calcium microfluorometry using the single-wavelength fluorescent Ca^{2+} indicator Fluo-4 AM (Life Technologies, Milan, Italy). Before measurements, high-density astrocytes seeded on O-CST devices pre-coated with PDL were loaded with $10 \text{ }\mu\text{M}$ Fluo-4 AM dissolved in standard bath solution for 30 min plus 15 min at room temperature. Samples were rinsed with standard bath solution after incubation. Measurements of $[\text{Ca}^{2+}]_i$ were performed by using a fluorescence microscope (Nikon Eclipse

Ti-S) equipped with long-distance dry objective (40x) and appropriate filters. The excitation wavelength was 470 nm with a light pulse duration of 200 ms and a sampling rate of 1.5 Hz. Complete data acquisition was controlled by MetaFluor software (Molecular Devices). Specific voltage protocols were applied to the O-CSTs and diodes by a custom-made 2612A Dual-channel System Source Meter Instrument (Keithley).

Blockers were diluted in standard bath saline to their respective final concentration and added after rinsing.^[35] The percentage (%) of inhibition of fluorescence emission was calculated as follows $[(F_{tcontrol}/F_{t0control} - F_{tblocker}/F_{t0blocker})/F_{tcontrol}/F_{t0control}] \times 100$, where $F_{tcontrol}/F_{t0control}$ was the fluorescence ratio F_t/F_{t0} recorded at the time points relative at the baseline (before the stimulation), at the end of stimulation and 50 s after the end of the stimulation, when we used standard bath solution containing calcium. The composition of bath solutions used is listed in session 2.7.

$F_{tblocker}/F_{t0blocker}$ was the fluorescence ratio F_t/F_{t0} recorded at the same time points relative at the baseline (before the stimulation), at the end of stimulation and 50 s after the end of the stimulation, when we use standard bath saline added with blocker or calcium-free extracellular solution.

2.6 Calcein self-quenching method. Cell-volume changes were monitored by Calcein fluorescence self-quenching method.^[36] Two days before the measurement, high-density astrocytes, seeded on O-CST devices coated with PDL, were loaded with 10 μ M Calcein-AM (Life Technologies, Milan, Italy) dissolved in standard bath solution for 15 min at room temperature.^[36] Complete data acquisition was controlled by the MetaFluor software. The excitation wavelength was 470 nm with a light pulse duration of 200 ms and a sampling rate

of 1.5 Hz. Specific voltage protocols were applied to the O-CST by a custom-made 2612A Dual-channel System Source Meter Instrument (Keithley).

2.7 Solutions and Chemicals. Salts and other chemicals were purchased of the highest purity grade from Sigma. For calcium microfluorometry experiments the standard bath solution was composed of (mM): 140 NaCl, 4 KCl, 2 MgCl₂, 2 CaCl₂, 10 HEPES, 5 glucose, pH 7.4 with NaOH and osmolarity adjusted to ~318 mOsm with mannitol.

Calcium-free extracellular saline contained (mM) 140 NaCl, 4 KCl, 4MgCl₂, 10 HEPES, 0.5 EGTA, pH 7.4 with NaOH and osmolarity adjusted to ~318 mOsm with mannitol.

Stock solutions of Gadolinium Chloride (Gd³⁺, 30 mM) and Ruthenium Red (RR, 10 mM), carbenoxolone (CBX, 50mM) and Brilliant Blue G (BBG, 10 mM) were prepared in water and stored at -20°C. Aliquots of RN-1734 (14.7 mM) and HC-030031 (40 mM) were prepared by dissolving in DMSO and stored at -20°C.

2.8 Simulations. Electrostatic potentials in O-CSTs were simulated by solving the Poisson equation on a 2D discretized model of the system. All geometrical parameters were taken from the experimental configuration, apart from top electrode lengths, reduced to 100 µm. Relative permittivity of materials was taken from the experiments (P13: 3.5, PMMA: 3.5, external solution: 80.0). Calculations were performed with the Sentaurus TCAD (Synopsys Inc.) software.

2.9 Statistical Analysis. Statistical analyses were performed by Origin 8.5. For calcium imaging experiments, the ratio of the fluorescence intensity at each time point (F_t) and the initial fluorescence (F_{t0}), that directly correlate with variation in $[Ca^{2+}]_i$ ^[37], was continuously recorded during the experiment. Data were compared by one-way ANOVA with Bonferroni

post-test. A statistically significant difference was reported if $p \leq 0.05$. Each data in the “Results and Discussion” section is presented as the mean \pm Standard Error (SE). Sample size (n) for each statistical analysis is reported in the Figure caption referred to the specific result. The data derived from at least 3 independent experiments performed at least in triplicate.

3. Results and discussion

3.1 P13 is a biocompatible substrate for the growth of primary astrocytes

The first step of our study was to test the biocompatibility of our O-CST with primary cortical astrocytes. In this view, we re-plated confluent astrocytes on P13 coated coverslips. After 2, 7 and 15 days *in vitro* (DIV) from re-plating, fluorescein diacetate (FDA) cell viability assays were performed. Single plane confocal imaging analyses depict viable astrocytes plated on both Glass+Poly-D-Lysine (PDL) and P13+PDL after 2 DIV (Figure 1A, B). Morphological observation revealed that a polygonal flat shape typical of *in vitro* cultured primary astrocytes^[38–40] was maintained in astrocytes plated on both PDL and P13+PDL. The histogram plot of cell counting at the chosen time points indicated that at 2 and 7 DIV the survival of astrocytes plated on P13+PDL was significantly higher compared to those observed on cells plated on PDL-coated glass. The number of cells was comparable in the two conditions after 15 DIV (Figure 1C). These data indicate the suitability of P13 as a biocompatible substrate for adhesion and growth of primary cortical astrocytes. These results confirmed and extended our previous study demonstrating that P13 is a biocompatible and thereby suitable substrate to be interfaced with neural cells.^[5] The results are also in line with previous studies showing that other organic materials, namely a mixture of poly(3-hexylthiophene) with phenyl-C61-butyric-acid-methyl ester (P3HT:PCBM), support the growth of pure primary cultured rat neocortical astrocytes better than control substrates.^[41] Indeed, it is widely recognized that chemical similarity between cell membrane and organic biointerface, as well as mechanical properties such as softness promote favourable interaction between organic materials and neural cells.^[42]



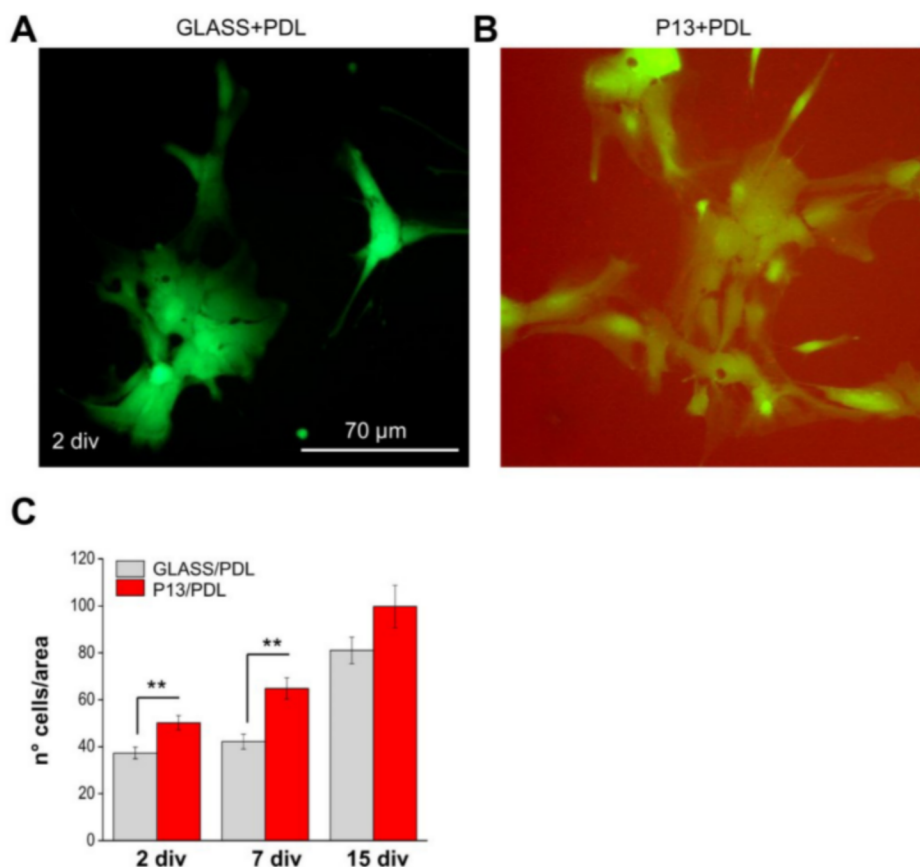


Figure 1. Viability of Astrocytes on the O-CST. Fluorescent micrographs representing astrocytes after 2 days in vitro (div) stained for fluorescein diacetate (FDA) on (A) Glass+PDL and (B) P13+PDL; the P13 film is imaged by the red detection channel. (C) Histogram plot of averaged FDA positive cells/area counted in astrocytes cell culture plated on Glass+PDL and P13+PDL, after 2, 7 and 15 div. A statistical difference was observed after 2 and 7 div (** $p < 0.01$, ANOVA one-way).

3.2 Extracellular electrical stimulation by O-CST elicits astrocytic intracellular Ca^{2+} increase

We next took advantage of the O-CST device transparency to study the effect of extracellular stimulation operating the organic transistor device at sub-threshold bias ($< 1\text{V}$) on astrocytic Ca^{2+} signalling. A scheme of the experimental setup is displayed in Figure 2A. We have loaded the cells with Fluo-4-AM and performed calcium imaging experiments, 48 h after the

re-plating of cells on O-CST in external standard solution containing Ca^{2+} (2 mM, Figure 2B). The stimulation protocol applied to the O-CST is reported in Figure 2C inset. It is important to highlight that the OCST is operated well below the bias conditions necessary for charge accumulation and transport in the transistor channel. The applied voltage is intended to provide the electrical stimulation at the top interface of the device suitable for cell stimulation, while avoiding generation of detrimental Faradaic currents.^[7] Gate Voltage (V_{GS}) was spanned from 0 to 1 V within a duration of 85 s at a rate of 11.76 mV/s, while Drain-Source Voltage (V_{DS}) was kept at 0 V (Figure 2C, inset). The total length of experiments was 300 s and O-CST stimulation was applied after 150 s of control recording (Figure 2C). The ratio of the fluorescence intensity at each time point (F_t) and the initial fluorescence (F_{t0}), that directly correlate with variation in $[\text{Ca}^{2+}]_i$ ^[37], was continuously recorded during the experiment. Figure 2C shows the typical response observed in the majority of the cells (Figure 2C, green trace) upon and after the application of the O-CST stimulation protocol, where F_t/F_{t0} value rises slowly but constantly over time. The histogram plot in Figure 2D is reporting the mean of F_t/F_{t0} values recorded before (Figure 2D white column), at the end of the stimulation (Figure 2D, red column) and 50 s after the end of O-CST operation (Figure 2D, blue column). The data revealed that, at the end of the stimulation, the F_t/F_{t0} value is increased of 30% with respect to the value recorded before the application of the stimulus. Then, F_t/F_{t0} continue to rise, reaching a value that was 50% higher with respect to the control, 50 s after the end of the stimulus. The effect of increase in calcium concentration elicited by O-CST was observed in the majority of the analysed cells (75.03 ± 7.71 %, Figure 2E). The fluorescent signal was stable over time, when cells grown on O-CST were monitored without

application of electrical stimulus (Supplementary Figure S1A). Accordingly, control experiments performed on cells grown on PDL coated glass coverslips confirmed that spontaneous activity occurs rarely in our experimental condition (Supplementary Figure S1B). Notably, the same stimulation protocol failed to elicit action potential when applied to Dorsal Root Ganglion primary neurons.^[7] We next sought to apply to astrocytes the pulsed stimulation protocols that were successfully applied to elicit action potential in neurons.^[7] The stimulation protocol consisted on a train of increasing pulsed voltages between the Gate and the Source (from $V_{GS}=0$ to $V_{GS}=1$ V) with linear increasing steps of 250 mV, a pulse duration of 10 ms and a frequency rate of 10ms, (inset to Figure Supplementary S2A). The total length of the stimulus was of 70 ms. We also applied a repetitive pulse stimulation protocol consisting on five times repetition of the train pulse stimulation described above, with a delay between episode of 10 ms (inset to Figure Supplementary S2B). The total stimulation length was 390 ms. Interestingly, the fluorescent signal was stable over time, when cells were stimulated either by one train of pulse (Figure S2 A) or by repetitive pulse train (Figure S2 B).

Collectively, these data indicated a direct correlation between O-CST stimulation and the observed effect of $[Ca^{2+}]_i$ increase. Moreover, they suggest that astrocytes and neurons respond differently to specific stimulation protocol. These results set the basis for cell specific neural stimulation studies by using O-CST.

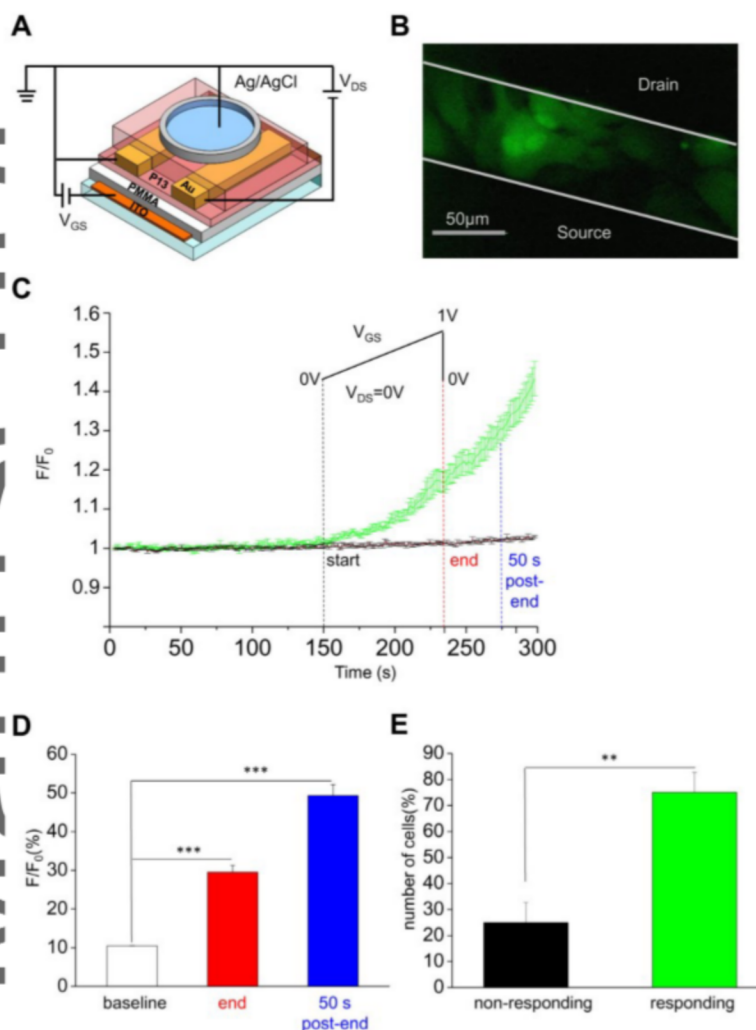
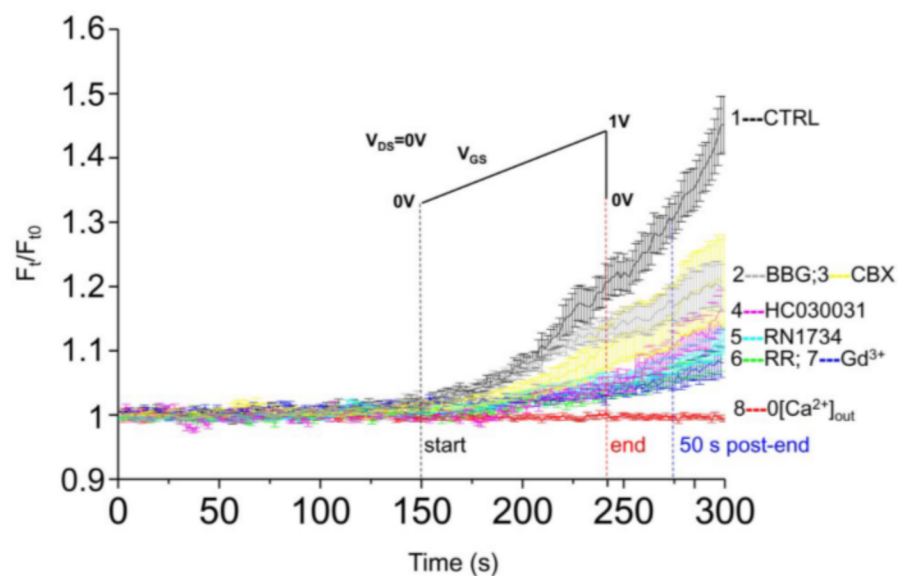
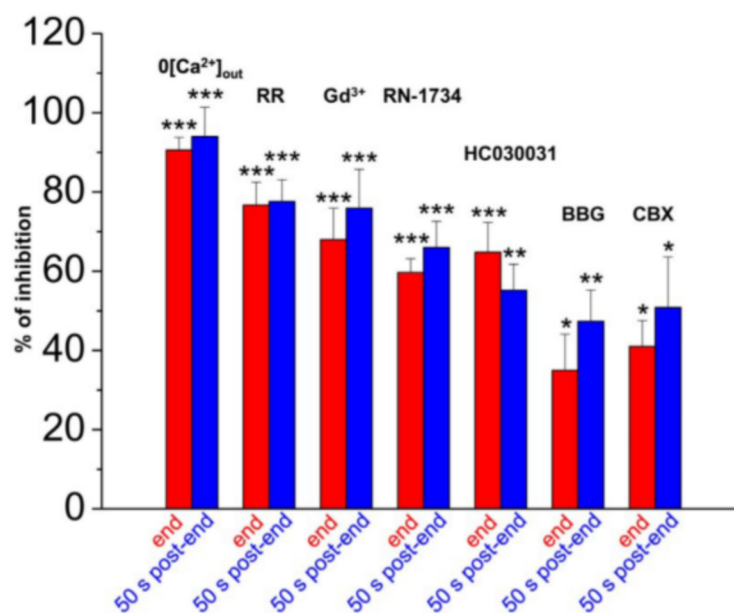


Figure 2. O-CST sub-threshold operation promotes $[Ca^{2+}]_i$ increase in astrocytes. (A) Schematic representation of calcium imaging experiment performed on cells plated and stimulated by O-CST device. (B) Fluorescent micrograph of cells labelled with Fluo-4 on O-CST device taken during one of the performed experiments. (C) Representative averaged trace with standard error (SE) of calcium imaging experiment on O-CST device. A transfer stimulation protocol with $V_{GS} = 0-1V$ and $V_{DS} = 0V$ with a duration of 85s was applied after 150s from the beginning of the experiment (black dashed bar). The end of the stimulation (red dashed bar) and 50 s after the end of the stimulation (blue dashed bar) where the time points used for the calculation (see Experimental Section) (F = fluorescence intensity; F_{t_0} = fluorescence intensity at time point = 0s). (D) Histogram plot depicting the averaged fluorescence intensity recorded before the stimulation (baseline, white column), at the end of the stimulation (red column) and 50s after the stimulation (blue column). The values are presented as mean with SE. A statistical difference can be observed between the value recorded at the control and at the end of the stimulation as well as at the control and 50s after the stimulation. (Baseline, $n=135$, end of the stimulation, $n=106$, 50s post-stimulation, $n=106$;

*** $p < 0.001$, One-way ANOVA). Results represent at least eight independent experiments performed in triplicate. (E) Histogram plot showing the percentage of cells non-responding (black bar) and responding (green bar) to electrical stimulation. The values are presented as mean with SE. Statistical significance can be observed between the number of responding and not responding cells. ($n=135$, ** $p < 0.01$, One-way ANOVA).

We next sought to verify the pharmacological profile of the $[Ca^{2+}]_i$ response promoted by O-CST operation. To verify the contribution of extracellular calcium influx in the O-CST mediated Ca^{2+} increase, we repeated the experiment exposing the cells to Ca^{2+} free external saline solution (Figure 3A, trace 8). Interestingly, under this experimental condition O-CST operation almost failed to evoke significant $[Ca^{2+}]_i$ response in stimulated astrocytes, compared to the effect observed in control solution (Figure 3 A, CTRL, trace 1, black). Indeed, the F/F_0 values recorded at the end of the stimulation (Figure 3B, red column) and 50 s after the O-CST operation, (Figure 3B, blue column) was almost completely inhibited ($90.58 \pm 3.19\%$, at the end of the stimulation and $94.02 \pm 7.335\%$ 50s after the stimulus) (Figure 3 A, $0[Ca^{2+}]_{out}$, trace 8, red). The data clearly indicated that extracellular calcium influx was essential for the observed effect.

A**B**

AL

Figure 3. TRPV4 mediates $[Ca^{2+}]_i$ increase in astrocytes elicited by O-CST device. A) Averaged traces with SE of calcium imaging experiments performed while stimulating cells on the O-CST channel using as bath: a control extracellular solution (CTRL, trace 1, black) and Ca^{2+} free external solution ($0[Ca^{2+}]_{out}$, trace 8, red) or a control extracellular solution added with Ruthenium Red (RR) (10 μ M, B, trace 6, green), Gadolinium Chloride (Gd^{3+} , 10 μ M, C, trace 7, dark blue), RN-1734 (10 μ M, D, trace 5, blue), HC-030031 (40 μ M, E, trace 4, purple), Brilliant Blue G (BBG, 10 μ M, F, trace 2, gray) Carbenoxolone (50 μ M, CBX, G, trace 3, yellow). H) Histogram plot showing the mean percentage inhibition of fluorescence intensity of the analysed cells at the end of the stimulation (red bars) and 50s after the stimulation (blue bars) normalized to the value recorded when the experiments were performed by using control solution (CTRL). (Ca^{2+} free external solution n=69, RR n=39, RN-1734 n=39, Gd^{3+} n=78, HC-030031 n=34, BBG n=76 and CBX n=52). The values are presented as mean with SE. Statistical significance were calculated with respect to the value recorded when the experiments were performed by using control solution (CTRL), considered as 100%. (** $p < 0.01$ ** $p < 0.01$ and * $p \leq 0.05$. One-way ANOVA). Results represent at least three independent experiments performed at least in triplicate.

Several studies indicated that in astrocytes, TRP channels are involved in extracellular Ca^{2+} entry into the cytosol, in response to physical stimuli such as mechanical, osmotic stress and temperature.^[43] To investigate the contribution of TRP channels in the observed effect, we applied non selective blockers of TRP family^[35,44] Ruthenium Red (10 μ M, RR, Figure 3A, trace 6, green) and Gadolinium Chloride (10 μ M, Gd^{3+} , Figure 3A, trace 7, dark blue). In both cases, we observed that, compared to the effect observed applying O-CST stimulation in standard control solution (Figure 3A, trace 1, black), a significant inhibition of F_i/F_{i0} occurred when RR and Gd^{3+} were added to the control solution. In particular, the inhibition was $76.68 \pm 5.81\%$ for RR and $67.93 \pm 7.95\%$ for Gd^{3+} at the end of the stimulation and $77.59 \pm 5.56\%$ for RR and $75.89 \pm 9.81\%$ for Gd^{3+} 50 after the end of the stimulation (Figure 3B). These results suggest that members belonging to TRP family might account for the observed $[Ca^{2+}]_i$ increase elicited by O-CST stimulation. Additionally, by application of selective TRPV4 antagonist RN-1734 (10 μ M, Figure 3A, trace 5, blue)^[45], the F_i/F_{i0} intensity was largely abolished, with respect to the control experiment performed in standard saline ($59.67 \pm 3.49\%$ at the end of the stimulation, Figure 3B, red column and $65.97 \pm 6.55\%$ 50 s after the end of

the stimulation, Figure 3B, blue column). Similarly, the addition of selective inhibitor of the channel TRPA1, the molecule HC 030031 (40 μ M, Figure 3A, trace 4, purple)^[19], strongly diminished the F_t/F_{t0} value ($64.77 \pm 7.60\%$ of inhibition at the end of the stimulation and $55.18 \pm 6.54\%$ of inhibition 50 seconds after the end of O-CST operation) in comparison to the value recorded when cells were exposed to CTRL solution. All these evidence indicated that TRPV4 and TRPA1 were majorly contributing to the $[Ca^{2+}]_i$ increase induced by O-CST stimulation.

To investigate the contribution of the P2X₇ receptor to the observed effect we add Brilliant Blue G (BBG)^[46], at a concentration of 10 μ M (Figure 3A, trace 2, grey) to the control solution (Figure 3A, trace 1, black) and we observed a significant inhibition of fluorescent increase ($34.97 \pm 9.10\%$ at the end of the stimulation and $47.35 \pm 7.89\%$ 50 s after the end of the stimulation). Moreover, using Carbenoxolone (CBX)^[47] (50 μ M, Figure 3A, trace 3, yellow), an inhibitor of gap junctional channels, connexins (Cx) and of pannexins (Panx), we also observed a lower but significant decrease in F_t/F_{t0} response evoked by O-CST ($40.99 \pm 6.57\%$ at the end of the stimulation and $50.82 \pm 12.76\%$ 50 s after gate off).

3.3 O-CST operation induces astrocytes swelling and preserves cell viability

It has been shown that application of extracellular electric field results in cell swelling in several cell types.^[48–51] The swelling magnitude was dependent on the duration of the stimulation and on the intensity of the applied field.^[48–51] We have previously demonstrated that TRPV4 is responsible for swelling induced extracellular Ca^{2+} influx in astrocytes.^[35,52] Recently, the involvement of TRPA1 in osmotic induced Ca^{2+} influx have been reported.^[53]

Thus, we hypothesized that electric field generated by O-CST might induce cell swelling and, in turn, activate calcium signalling in astrocytes via TRPV4 and TRPA1. Since it is well-known that alteration of Ca^{2+} homeostasis can lead to cell death, we performed FDA cell viability assay 24h after device operation. Confocal imaging and cell counting were performed in cells non-stimulated (Figure 4C) and stimulated (Figure 4D) revealing that astrocytes are still viable on the O-CST, 24h after device operation. Moreover, cell counting revealed that the number of astrocytes/area was not significantly different between stimulated and non-stimulated cells (Figure 4E).

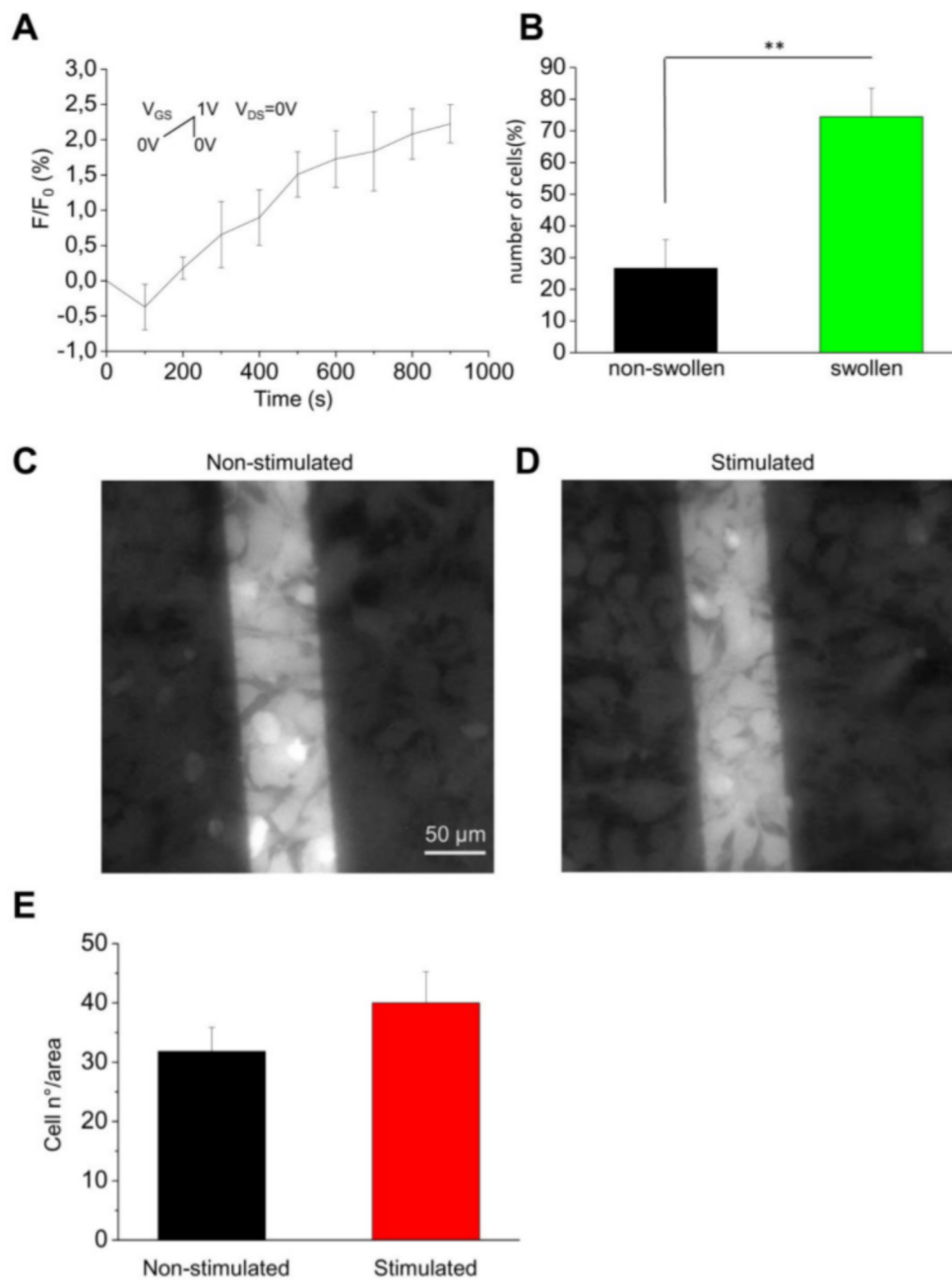


Figure 4. O-CST operation induces astrocytes swelling and doesn't alter cell viability. (A) Calcein self-quenching method for measurement of osmotically induced volume changes in primary astroglial cells. Time course of the percentage increase of fluorescence intensity of calcein before, during and after O-CST stimulation (inset reported above the graph). An increase

in fluorescence intensity represents cell swelling. Results are representative of at least five independent experiments (n=42). (B) Histogram plot depicting the percentage of cells swollen (green) and non-swollen (black) to stimulation. The values are presented as mean with SE. Statistical significance can be reported between the number of swollen and non-swollen cells. (** p<0.01. One-way ANOVA. n=56) (C) Fluorescence images showing FDA staining and viable cells 48h after plating on the O-CST and (D) 48h after plating and 24h after device operation (top contacts of the O-CST in dark). E) Histogram plot showing the average FDA positive cells/area. Astrocytes were plated on the device and images were taken 24h after the stimulation (red). The second group of samples treated under the same condition was not stimulated and used as control (black). No statistical difference was observed. Results represent mean \pm SE collected from three independent experiments (n=30, p>0.05, ANOVA one-way).

To verify this hypothesis, we performed cell volume measurements in astrocytes exposed to O-CST stimulation, by performing calcein self-quenching method.^[36] We could observe that in response to O-CST stimulation (Figure 4A), an increase in Calcein fluorescence occurs over time, reaching the value of 2% few minutes after cell stimulation. According to previous studies the observed increase corresponds to a significant increase in cell volume (cell swelling).^[36] The swelling occurred in the majority of cells ($74.40 \pm 9.02\%$, Figure 4B).

The data we provided clearly indicated that O-CST is capable to stimulate astrocytes Ca^{2+} increase, by slow and sub-threshold voltage ramp. The pharmacological analyses provided here revealed that two members of the TRP family, TRPV4 and TRPA1 are majorly involved in the Ca^{2+} increase promoted by O-CST stimulation.

TRPV4 is a non-selective cation channel with a high permeability for Ca^{2+} and for monovalent cations.^[54] TRPV4 in the cortex is majorly expressed in astrocytes.^[18,19] In vitro and in situ data revealed that astrocytic TRPV4 is activated by a variety of stimuli, including increase in temperature ^[55], osmotic stress and cell swelling ^[35], volume changes ^[56], and agonist such as 4α -phorbol 12,13-didecanoate, 4α PDD.^[18,35] TRPV4 channels can be triggered by increase in $[\text{Ca}^{2+}]$, and it stimulates Ca^{2+} -induced Ca^{2+} release in astrocytic endfeet, amplifying neurovascular coupling responses.^[57]

Aut

Regarding the possible mechanism of TRP activation, we observed that O-CST stimulation induce moderate but significant cell swelling that last over several minutes after stimulus end. A recent computational study showed that upon application of external electric fields, water dipole orientation is affected within the region of the channels pore, modifying human AQP4 water permeability.^[58] In this view, we can hypothesize that the external electric field generated by O-CST operation, might induce AQP4 dependent cell swelling, and in turn promote TRPV4 activation.^[35] Futures studies on AQP4 KO models will clarify this aspect. Nevertheless, given the fact that TRP channels are polymodal channels, it cannot be ruled out that thermal dispersion or capacitive charging at the interface induced by the electric field could trigger TRPV4 and TRPA1 activation.

Author Manuscript

In astrocytes, TRPV4 is known to interact with Aquaporin-4 (AQP4) and to play a role in cell volume regulation.^[35] TRPA1 is also a non-selective cation channel that is permeable to Ca^{2+} , Na^{+} and K^{+} .^[59] TRPA1 is expressed in astrocytes and it is implicated in the control of basal levels of $[\text{Ca}^{2+}]_i$ ^[60] triggering the release and uptake of neurotransmitters, such as D-serine and GABA.^[61] Interestingly, TRPV4 is up-regulated in astrocytes following ischemia in a rat model of middle cerebral aortic occlusion.^[44] Moreover, the over expression and altered cellular distribution of TRPV4 was observed in autptic samples from patients suffering of Focal Cortical Dysplasia (FCD), a well-known cause of medically intractable epilepsy.^[62] All these evidences highlight the relevance of our finding and the potential application of using O-CST stimulation in neurophysiology. Moreover, the data presented here, combined with those of our previous work^[7], indicate that the same organic device might be used for selective stimulation of astrocytes or neurons depending on the need, by changing the bias applied between the three electrodes. In perspective, O-CST stimulation might be a potential way to target TRP channels and prevent/cure acute neuropathologies.

The implication of P2X_7 and gap junction channels was also suggested by the reported results. We observed also that CBX and BBG inhibit the $[\text{Ca}^{2+}]_i$ increase induced by O-CST operation. The effect of BBG and CBX might be explained by involvement of P2X_7 and Cx or Panx in the observed effect. However, due to the low selectivity of the pharmacological agent ^[47,63], the contribution of these channels will need further investigations.



3.4 O-CST device architecture enable calcium signalling

In order to investigate the role of the O-CST architecture in the observed effect, we performed calcium imaging experiments by using a diode structure with only one gold electrode and P13 as semiconductor and capping layer (Figure 5A), instead of the O-CTS three electrode transistor architecture. We could observe that by operating the diode device with the same linear ramp stimulation previously applied to the gate of the O-CST (in the case of the diode, from 0 V to 1 V applied to the gold electrode with respect to the reference electrode in the bath), failed to evoke any response in the majority of cells ($98.57 \pm 1.42\%$, Figure 5D). Indeed, the fluorescence intensity remained unchanged before stimulation, during the stimulation and 50 seconds after diode operation (Figure 5C).

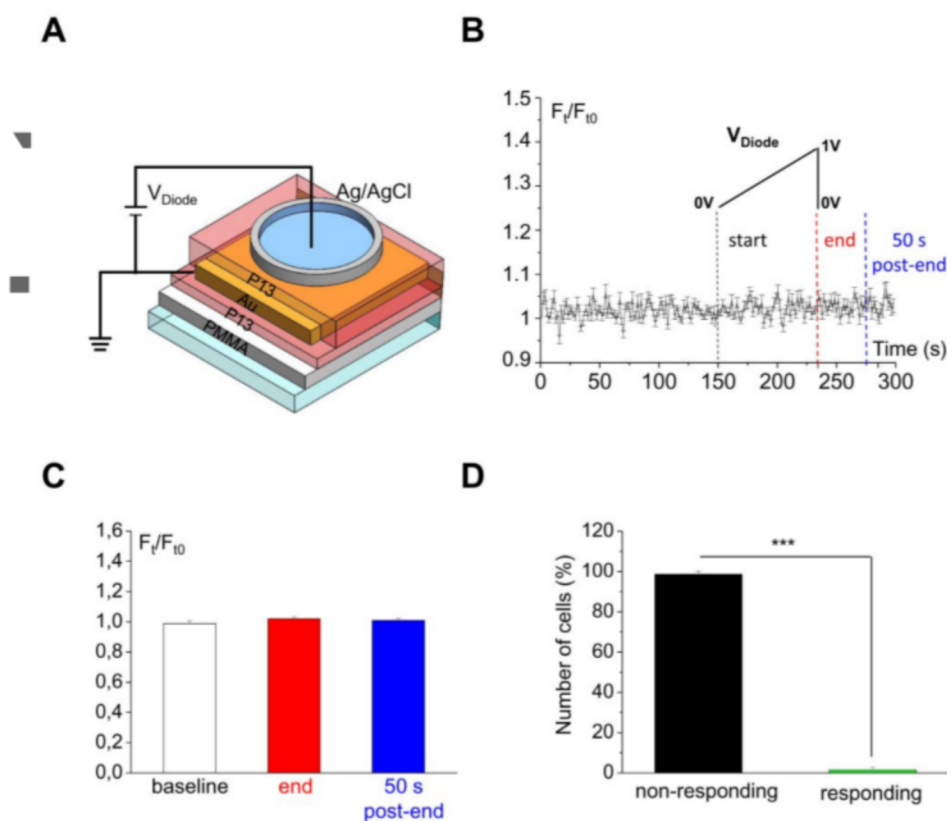


Figure 5. Cellular response in dependence of the device architecture. (A) Representation of the diode device structure and voltage application protocol (V_{Diode} from 0 to 1V). (B) Representative averaged trace \pm SE of calcium imaging experiment performed on cells plated on a diode. A continuous stimulation protocol with a duration of 85 s was applied at 150 s (black dashed bar). The voltage between the electrode and the solution (V_{Diode}) goes from 0 to 1 V as depicted in the inset. The stimulation duration was 85s, as depicted by indication of stimulation end (red dashed bar). (C) Histogram plot depicting the mean fluorescence before stimulation (baseline, white column), end of the stimulation (red column) and 50s after the end of the stimulation (blue column). Results represent at least ten independent experiments. (D) Histogram plot showing the percentage of cells non-responding and responding to the stimulation. The values are presented as mean with SE. A statistical difference can be reported between the number of responding and non-responding cells ($n=115$, *** $p<0.001$. One-way ANOVA).

We further investigated the impact of the O-CST structural integrity and device working functionality on the astrocytic response. Figure 6 reports typical gate current of an undamaged O-CST and of an O-CST with a leaking dielectric, recorded upon the stimulation protocol reported above. The undamaged O-CST device has a maximum leakage current of 2

nA (red circles) whereas the device with leaking dielectric shows a thousand-fold higher leakage current of about 2 μ A (black squares). Calcium imaging experiments, applying the same protocol reported in Figure 2A, on an O-CST device with a gate leakage-current of 2 μ A, revealed that a leaking device fails to evoke $[Ca^{2+}]_i$ signal in astrocytes (Figure 6 B, black trace). On the contrary, the O-CST operation successfully stimulates increase in $[Ca^{2+}]_i$ when the device has a maximum leakage current of 2 nA (Figure 6B, red trace). These results show that O-CST architecture and integrity are essential for its ability to evoke $[Ca^{2+}]_i$ on astroglial cells and confirm that the cell stimulation is due to a capacitive effect between the ITO electrode and the organic-solution interface. Indeed, only the undamaged O-CST where the leakage current is practically absent, and the field effect is preserved can evoke cell response, while the device with defective dielectric and resistive behaviour between the ITO electrode and the organic-solution interface cannot.

The mechanism of localized stimulation of cells through extracellular electric fields was analyzed by modelling the electrostatic potential distribution in an O-CST configuration (Figure 6D). The working mechanism of the device might be related to the capacitive coupling enabled by close interaction and proximity between the organic layer and the cellular membrane. By applying a small positive (1 V) bias to the back electrode and grounding the two top electrodes, the electrostatic potential is null above the electrodes and about 0.7 V in the region above the channel. Therefore, the O-CST configuration is able to induce a relatively large potential in a localized region of space (see Figure 6E). A regular increase of V_b over time is thus potentially able to realize a steady variation of the potential at the organic-solution interface from 0 to about 0.7 V. Indeed, the physical-chemical affinity

and the close proximity between the functionalized organic layer and the cellular membrane is believed to create a direct contact between the device and the membrane ion channel. The morphology and the properties of the bio-organic interface realized constitute thus a crucial prerequisite to efficient stimulation. The mechanism for stimulation can therefore be related to the peculiar architecture of the O-CST device, which couples the formation of a stable bio-organic interface, between the cell membrane and the organic layer, with the development of electric fields across the organic thin-film.

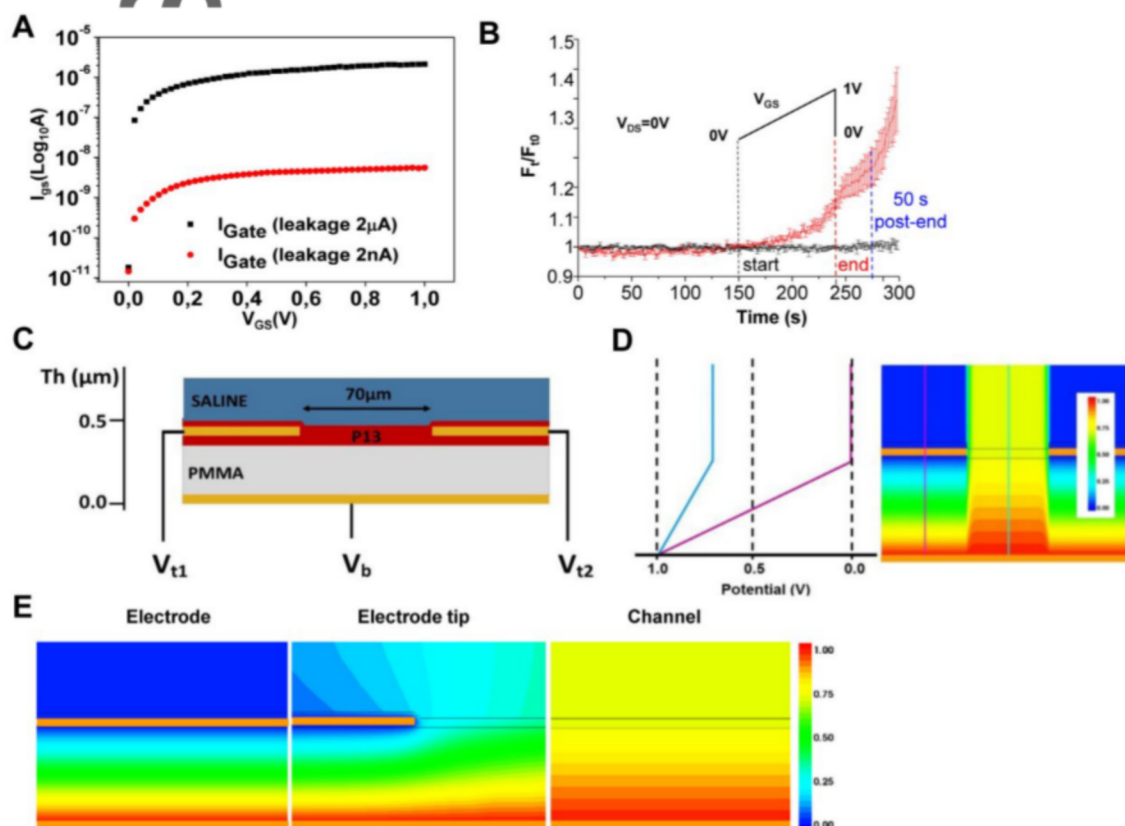


Figure 6. O-CST architecture and structural integrity are essential for cellular response. (A) Gate current plots in an O-CST with minimum leakage current (red trace) in comparison to a device with a high leakage of 2 μA (black trace). (B) Average traces \pm SE of calcium imaging experiment on O-CST device with a leakage current of 2 μA (black trace) and 2 nA (red

trace). A continuous stimulation protocol with duration of 85 s was applied at 150 s. (C) Representation of the device model system (not to scale; x:y=1:100). (D) Computed electrostatic potential at $V_b=1.0$ V and $V_{t1}=V_{t2}=0$ along two vertical cuts (magenta: electrode; cyan: channel) across the device (x:y=1:200). (E) Distribution of the electrostatic potential at $V_b=1.0$ V; $V_{t1}=V_{t2}=0$ in different zones of the device (x:y=1:1). Values in the scalebar are in Volt.

4. Conclusions

We report the first evidence of an organic semiconductor device capable to modulate functional properties of non-excitable astroglial cells by applying extracellular electric field. We found that the contribution of TRP family member, TRPV4 and TRPA1 is essential. Notably the O-CST device architecture is essential for successful stimulation of astrocytes.

In our previous study, we have demonstrated that astroglial chloride conductance can be modulated *in vitro* by photostimulation of P3HT/PCBM-ITO hybrid solid liquid interface.^[41] Also, a previous work reported on the use of organic electronic ion pump to release glutamate locally, that in turn, stimulate astrocytes calcium signalling.^[64] The present work reports for the first time on the effect of the electric field produced by an organic semiconductor device on astrocytes calcium signalling. In this view, by showing the ability of O-CST to evoke calcium signal in astrocytes, we add a substantial piece of evidence on the potential of organic bioelectronics to modulate astrocytes functionality. Considering the pivotal role of astrocytes in the physiology and pathology of the brain, our results open the way for the development of novel bioelectronic approaches targeting glial cells as main factor in brain functionality.

Acknowledgements

This work was supported by EU Marie Curie Project OLIMPIA (GA 316832) and by the AFOSR Research Projects ASTROMAT, FA9550 16-1-0502 and ASTRONIR, FA9550-17-1-0502. We are grateful to Vincenzo Ragona from CNR-ISMN and Ilja Grishin and Sebastien Pecqueur from E. T. C. S.r.l. for their support in device fabrication and Paolo Mei from CNR-ISMN for his technical assistance. We are grateful to Dr Alessia Minardi from FABIT Dept. of the University of Bologna, for her help in the preparation and maintenance of astrocytes primary culture.

References

- [1] V. Benfenati, K. Stahl, C. Gomis-Perez, S. Toffanin, A. Sagnella, R. Torp, D. L. Kaplan, G. Ruani, F. G. Omenetto, R. Zamboni, M. Muccini, *Adv. Funct. Mater.* **2012**, 22, 1871.
- [2] M. Berggren, A. Richter-Dahlfors, *Adv. Mater.* **2007**, 19, 3201.
- [3] D. Khodagholy, T. Doublet, P. Quilichini, M. Gurfinkel, P. Leleux, A. Ghestem, E. Ismailova, T. Hervé, S. Sanaur, C. Bernard, G. G. Malliaras, *Nat. Commun.* **2013**, 4, DOI 10.1038/ncomms2573.
- [4] D. Ghezzi, M. R. Antognazza, M. Dal Maschio, E. Lanzarini, F. Benfenati, G. Lanzani, *Nat. Commun.* **2011**, 2, 164.

- [5] S. Toffanin, V. Benfenati, A. Pistone, S. Bonetti, W. Koopman, T. Posati, A. Sagnella, M. Natali, R. Zamboni, G. Ruani, M. Muccini., *J. Mater. Chem. B* **2013**, *1*, 3850.
- [6] S. Bonetti, A. Pistone, M. Brucale, S. Karges, L. Favaretto, M. Zambianchi, T. Posati, A. Sagnella, M. Caprini, S. Toffanin, R. Zamboni, N. Camaioni, M. Muccini, M. Melucci, V. Benfenati, *Adv. Healthc. Mater.* **2015**, *4*, 1190.
- [7] V. Benfenati, S. Toffanin, S. Bonetti, G. Turatti, A. Pistone, M. Chiappalone, A. Sagnella, A. Stefani, G. Generali, G. Ruani, D. Saguatti, R. Zamboni, M. Muccini, *Nat. Mater.* **2013**, *12*, 672.
- [8] B. Han, Y. Huang, R. Li, Q. Peng, J. Luo, K. Pei, A. Herczynski, K. Kempa, Z. Ren, J. Gao, *Nat. Commun.* **2014**, *5*, 1.
- [9] O. Ostroverkhova, *Chem. Rev.* **2016**, *116*, 13279.
- [10] V. Benfenati, S. Ferroni, *Neuroscience* **2010**, *168*, 926.
- [11] A. Araque, G. Perea, *Glia* **2004**, *47*, 241.
- [12] A. Verkhratsky, M. Nedergaard, *Physiol. Rev.* **2018**, *98*, 239.
- [13] M. Navarrete, G. Perea, L. Maglio, J. Pastor, R. García De Sola, A. Araque, *Cereb. Cortex* **2013**, *23*, 1240.
- [14] E. Scemes, C. Giaume, *Glia* **2006**, *54*, 716.
- [15] L. Leybaert, M. J. Sanderson, *Physiol. Rev.* **2012**, *92*, 1359.

- [16] A. Volterra, N. Liaudet, I. Savtchouk, *Nat. Rev. Neurosci.* **2014**, *15*, 327.
- [17] P. Ballerini, R. Ciccarelli, F. Caciagli, M. P. Rathbone, E. S. Werstiuk, U. Traversa, S. Buccella, P. Giuliani, S. Jiang, E. Nargi, D. Visini, C. Santavenere, P. Di Iorio, *Int. J. Immunopathol. Pharmacol.* **2005**, *18*, 417.
- [18] V. Benfenati, M. Amiry-Moghaddam, M. Caprini, M. N. Mylonakou, C. Rapisarda, O. P. Ottersen, S. Ferroni, *Neuroscience* **2007**, *148*, 876.
- [19] E. Shigetomi, X. Tong, K. Y. Kwan, D. P. Corey, B. S. Khakh, *Nat. Neurosci.* **2012**, *15*, 70.
- [20] S. Ben Achour, L. Pont-Lezica, C. Béchade, O. Pascual, *Neuron Glia Biol.* **2010**, *6*, 147.
- [21] G. Perea, M. Navarrete, A. Araque, *Trends Neurosci.* **2009**, *32*, 421.
- [22] G. Dallérac, N. Rouach, *Prog. Neurobiol.* **2016**, *144*, 48.
- [23] J. J. Rodríguez, M. Olabarria, A. Chvatal, A. Verkhratsky, *Cell Death Differ.* **2009**, *16*, 378.
- [24] L. Tian, G. Or, Y. Wang, G. Shi, Y. Wang, J. Sun, S. Papadopoulos, G. Broussard, E. Unger, W. Deng, J. Weick, A. Bhattacharyya, C. Y. Chen, G. Yu, L. L. Looger, L. Tian, *bioRxiv* **2018**, *24*, 247585.
- [25] G. Carmignoto, P. G. Haydon, *Glia* **2012**, *60*, 1227.

- [26] R. J. Molenaar, *ISRN Neurol.* **2011**, 2011, 1.
- [27] S. Ding, *Adv Neurobiol.* **2014**, 11, 189.
- [28] H. Monai, M. Ohkura, M. Tanaka, Y. Oe, A. Konno, H. Hirai, K. Mikoshiba, S. Itohara, J. Nakai, Y. Iwai, H. Hirase, *Nat. Commun.* **2016**, 7, 1.
- [29] E. Wanke, F. Gullo, E. Dossi, G. Valenza, A. Becchetti, *J. Neurophysiol.* **2016**, 116, 2706.
- [30] P. R. F. Rocha, M. C. R. Medeiros, U. Kintzel, J. Vogt, I. M. Araújo, A. L. G. Mestre, V. Mailänder, P. Schlett, M. Dröge, L. Schneider, F. Biscarini, D. M. de Leeuw, H. L. Gomes, *Sci. Adv.* **2016**, 2, 1.
- [31] W. Fleischer, S. Theiss, J. Slotta, C. Holland, A. Schnitzler, *Physiol. Rep.* **2015**, 3, 1.
- [32] A. L. G. Mestre, P. M. C. Inácio, Y. Elamine, S. Asgarifar, A. S. Lourenço, M. L. S. Cristiano, P. Aguiar, M. C. R. Medeiros, I. M. Araújo, J. Ventura, H. L. Gomes, *Front. Neural Circuits* **2017**, 11, 1.
- [33] S. Ferroni, C. Marchini, P. Schubert, C. Rapisarda, *FEBS Lett.* **1995**, 367, 319.
- [34] V. Benfenati, M. Caprini, G. P. Nicchia, A. Rossi, M. Dovizio, C. Cervetto, M. Nobile, S. Ferroni, *Channels* **2009**, 3, DOI 10.4161/chan.3.5.9568.
- [35] V. Benfenati, M. Caprini, M. Dovizio, M. N. Mylonakou, S. Ferroni, O. P. Ottersen, M. Amiry-Moghaddam, *Proc. Natl. Acad. Sci.* **2011**, 108, 2563.

- [36] E. Solenov, *AJP Cell Physiol.* **2004**, 286, 426C.
- [37] M. D. Bootman, K. Rietdorf, T. Collins, S. Walker, M. Sanderson, *Cold Spring Harb. Protoc.* **2013**, 8, 83.
- [38] V. Benfenati, M. Caprini, M. Nobile, C. Rapisarda, S. Ferroni, *J. Neurochem.* **2006**, 98, 430.
- [39] T. Posati, A. Pistone, E. Saracino, F. Formaggio, M. G. Mola, E. Troni, A. Sagnella, M. Nocchetti, M. Barbalinardo, F. Valle, S. Bonetti, M. Caprini, G. P. Nicchia, R. Zamboni, M. Muccini, V. Benfenati, *Sci. Rep.* **2016**, 6, 1.
- [40] V. Benfenati, S. Toffanin, R. Capelli, L. M. A. Camassa, S. Ferroni, D. L. Kaplan, F. G. Omenetto, M. Muccini, R. Zamboni, *Biomaterials* **2010**, 31, 7883.
- [41] V. Benfenati, N. Martino, M. R. Antognazza, A. Pistone, S. Toffanin, S. Ferroni, G. Lanzani, M. Muccini, *Adv. Healthc. Mater.* **2014**, 3, 392.
- [42] P. Fattahi, C. E. Departments, P. State, G. Yang, G. Kim, **2014**, 26, 1846.
- [43] A. Verkhratsky, R. C. Reyes, V. Parpura, *Rev. Physiol. Biochem. Pharmacol.* **2013**, DOI 10.1007/112.
- [44] O. Butenko, D. Dzamba, J. Benesova, P. Honsa, V. Benfenati, V. Rusnakova, S. Ferroni, M. Anderova, *PLoS One* **2012**, 7, DOI 10.1371/journal.pone.0039959.
- [45] F. Vincent, A. Acevedo, M. T. Nguyen, M. Dourado, J. DeFalco, A. Gustafson, P. Spiro, D. E. Emerling, M. G. Kelly, M. A. J. Duncton, *Biochem. Biophys. Res. Commun.*

2009, 389, 490.

- [46] L. H. Jiang, a B. Mackenzie, R. a North, a Surprenant, *Mol. Pharmacol.* **2000**, 58, 82.
- [47] R. Iglesias, G. Dahl, F. Qiu, D. C. Spray, E. Scemes, *J. Neurosci.* **2009**, 29, 7092.
- [48] R. Strotmann, C. Harteneck, K. Nunnenmacher, G. Schultz, T. D. Plant, *Nat. Cell Biol.* **2000**, 2, 695.
- [49] W. Liedtke, Y. Choe, M. A. Martí-Renom, A. M. Bell, C. S. Denis, AndrejŠali, A. J. Hudspeth, J. M. Friedman, S. Heller, *Cell* **2000**, 103, 525.
- [50] S. K. W. Chang, *IEEE Trans. Biomed. Eng.* **1993**, 40, 1054.
- [51] O. M. Nesin, O. N. Pakhomova, S. Xiao, A. G. Pakhomov, *Biochim. Biophys. Acta - Biomembr.* **2011**, 1808, 792.
- [52] M. G. Mola, A. Sparaneo, C. D. Gargano, D. C. Spray, M. Svelto, A. Frigeri, E. Scemes, G. P. Nicchia, *Glia* **2016**, 64, 139.
- [53] F. Fujita, K. Uchida, Y. Takayama, Y. Suzuki, M. Takaishi, M. Tominaga, *J. Physiol. Sci.* **2017**, 1.
- [54] T. Voets, J. Prenen, J. Vriens, H. Watanabe, A. Janssens, U. Wissenbach, M. Bödding, G. Droogmans, B. Nilius, *J. Biol. Chem.* **2002**, 277, 33704.
- [55] K. Shibasaki, K. Ikenaka, F. Tamalu, M. Tominaga, Y. Ishizaki, *J. Biol. Chem.* **2014**,

289, 14470.

- [56] T. L. Tofte-Bertelsen, B. R. Larsen, N. MacAulay, *Channels* **2018**, *12*, 00.
- [57] K. M. Dunn, D. C. Hill-Eubanks, W. B. Liedtke, M. T. Nelson, *Proc. Natl. Acad. Sci.* **2013**, *110*, 6157.
- [58] J. A. Garate, N. J. English, J. M. D. MacElroy, *J. Chem. Phys.* **2011**, *134*, DOI 10.1063/1.3529428.
- [59] B. Nilius, V. Flockerzi, in *Handb. Exp. Pharmacol.*, **2014**.
- [60] E. Shigetomi, X. Tong, K. Y. Kwan, D. P. Corey, S. Baljit, **2012**, *15*, 70.
- [61] E. Shigetomi, O. Jackson-Weaver, R. T. Huckstepp, T. J. O'Dell, B. S. Khakh, *J. Neurosci.* **2013**, *33*, 10143.
- [62] X. Chen, F.-J. Sun, Y.-J. Wei, L.-K. Wang, Z.-L. Zang, B. Chen, S. Li, S.-Y. Liu, H. Yang, *Neurosci. Ther.* **2016**, *22*, 280.
- [63] V. Benfenati, M. Caprini, G. P. Nicchia, A. Rossi, M. Dovizio, C. Cervetto, M. Nobile, S. Ferroni, *Channels* **2009**, *3*, 323.
- [64] D. T. Simon, E. W. H. Jager, K. Tybrandt, K. C. Larsson, S. Kurup, A. Richter-Dahlfors, M. Berggren, *TRANSDUCERS 2009 - 15th Int. Conf. Solid-State Sensors, Actuators Microsystems* **2009**, 1790.

Intracellular calcium signalling ($[Ca^{2+}]_i$) of non-excitabile brain cells called astrocytes plays a pivotal role in brain function and dysfunction. Here, an organic transistor device architecture, named O-CST, is used to stimulate astrocytes $[Ca^{2+}]_i$. Sub-threshold voltages operation of O-CST induces astrocytes $[Ca^{2+}]_i$, largely mediated by TRP channels. Our result open the view for the use of organic devices to alter the functionality non-excitabile brain cells, by extracellular electric field.

Keyword: Organic bioelectronic

